# Development of Nanostructured Polyaniline–Titanium Dioxide Gas Sensors for Ammonia Recognition

**S. G. Pawar,[1] M. A. Chougule,[1] Shashwati Sen,[2] V. B. Patil[1]**

[1]*Materials Research Laboratory, School of Physical Sciences, Solapur University, Solapur (MS), India*
[2]*Crystal Technology Section, Technical Physics Division, Bhabha Atomic Research Centre, Mumbai, India*

Received 8 June 2011; accepted 20 June 2011
DOI 10.1002/app.35468
Published online 14 January 2012 in Wiley Online Library (wileyonlinelibrary.com).

**ABSTRACT:** The performance at room temperature of nanostructured polyaniline (PANi)–titanium dioxide ($TiO_2$) ammonia gas sensors was investigated. The PANi–$TiO_2$ thin-film sensors were fabricated with a spin-coating method on glass substrates. PANi–$TiO_2$ (0–50%) sensor films were characterized for their structural, morphological, optical, and various gas-sensing properties. The structural analysis showed the formation of nanocrystalline $TiO_2$, whereas PANi exhibited an amorphous nature. Morphological analysis of the PANi–$TiO_2$ nanocomposites film revealed a uniform distribution of $TiO_2$ nanoparticles in the PANi matrix. The absorption peaks in the Fourier transform infrared spectra and ultraviolet–visible spectra of the PANi–$TiO_2$ composite film were found to shift to higher wave numbers compared to those observed in pure PANi. The observed shifts were attributed to the interaction between the $TiO_2$ particles and the PANi molecular chains. The gas-sensing properties showed that the sensors exhibited selectivity to ammonia ($NH_3$) at room temperature. © 2012 Wiley Periodicals, Inc. J Appl Polym Sci 125: 1418–1424, 2012

**Key words:** conducting polymers; films; FT-IR; nanocomposites; sensors

## INTRODUCTION

Many studies of various materials as gas sensors have been reported in recent years. Gas-sensing materials can be classified mainly into two types: organic and inorganic materials. In recent years, the demand for gas sensors for safety control requirements and environmental monitoring has expanded enormously. The choice of a suitable sensing material along with efficient microelectronics for the detection system is a key step in such efforts.[1] The use of conducting polymers as sensing elements in chemical sensors has attracted attention because of their high sensitivity to changes in the electrical and optical properties when they are exposed to different types of gases or liquids. The ease in the synthesis of these polymers and sensitivity at room temperature add to the sensor's advantages. This can be of importance, particularly as ammonia sensors, which are used in different applications, such as in industrial processes, fertilizers, food technology, clinical diagnoses, farms, and environmental pollution monitoring.[2] Polyaniline (PANi) is one of the most attractive materials among the variety of conducting polymers because of its unique electrical properties, environmental stability, easy fabrication process, and intrinsic redox reaction.[3–5] PANi has also been used in different applications, including as light-emitting diodes,[6] rechargeable batteries,[7] and photovoltaic cells.[8] However, the problems with these conducting polymers are their low processing ability and poor chemical stability and mechanical strength.[9] There is a tremendous need for the enhancement of the mechanical strength and characteristics of sensors through the combination of organic materials with inorganic counterparts to form composites.[10,11] Accordingly, organic–inorganic nanocomposite sensors have been developed by several research groups. Among the inorganic materials, nanocrystalline titanium dioxide ($TiO_2$) is one of the most attractive and extensively used materials for the detection of $H_2$, liquefied petroleum gas (LPG), $NO_2$, and $NH_3$ gases.[12] A PANi/$SnO_2$ hybrid material was prepared by a hydrothermal method and studied for the gas sensing of ethanol and acetone by Geng et al.[13] Parvatikar et al.[14] fabricated PANi/tungsten oxide ($WO_3$) composite based sensors and reported that the film conductivity increased with increasing humidity. Dhawale et al.[12] fabricated PANi–$TiO_2$ heterostructural gas sensors for liquefied petroleum gas (LPG) sensing. Tai and coworkers[15,16] fabricated a PANi–$TiO_2$ nanocomposite for $NH_3$ and CO and reported that the films showed superior responses for $NH_3$ gas compared to CO. In this study, we carried out the *in situ* polymerization of

*Correspondence to:* V. B. Patil (drvbpatil@gmail.com).
Contract grant sponsor: Department of Science and Technology, New Delhi; contract grant number: SR/FTP/PS-09/2007.

PANi in the presence of $TiO_2$ nanoparticles on the sensor substrate at different temperatures. The main drawback of this process was that we could not control the amount of $TiO_2$ nanoparticles going into the film. In case of nanocomposites, the ratio of the organic to inorganic plays important roles in the morphology and the gas-sensing properties. Because PANi is a *p*-type semiconductor and $TiO_2$ is *n*-type in nature, their composite is expected to show *p–n* diode characteristics, as reported by Gong et al.[17] Thus, the electrical characteristics will be modulated by the ratio of PANi and $TiO_2$.

In this article, we report nanostructured PANi–$TiO_2$ (0–50%) thin-film gas sensors working at room temperature. The PANi–$TiO_2$ nanocomposites were prepared by the addition of $TiO_2$ at different weight percentages (0–50 wt %) to the PANi matrix. The nanocomposites were characterized by X-ray diffraction (XRD) in the 2θ range 10–70° with an X-ray diffractometer (Philips PW 3710, Almelo, Holland). Fourier transform infrared (FTIR) spectroscopy (PerkinElmer-100, Santa Clara, California, USA) was studied in the frequency range 400–4000 $cm^{-1}$. A morphological study of the PANi/$TiO_2$ (0–50 wt %) composite films was carried out with scanning electron microscopy (JEOL JSM 6360, Tokyo, Japan, operating at 20 kV). Optical measurements were carried out with a double-beam Simandzu-100 ultraviolet–visible (UV–vis) spectrophotometer (Kyoto, Japan). The gas-sensing measurements were made with a gas sensor set up at room temperature. The cross-sensitivity of the sensor to various gases was studied, and the sensor was found to be selective to ammonia.

## EXPERIMENTAL

### Synthesis of PANi

PANi was synthesized by the polymerization of aniline in the presence of hydrochloric acid as a catalyst and ammonium peroxidisulfate as an oxidant by the chemical oxidative polymerization method.[18]

### Synthesis of the $TiO_2$ nanoparticles

Nanocrystalline $TiO_2$ was synthesized by the sol–gel method with titanium isopropoxide as a source of Ti. The obtained powder was annealed in a tubular furnace at 700°C for 1 h to get $TiO_2$ nanopowder with particles at a size of 50–60 nm.[19]

### Synthesis of the PANi–$TiO_2$ nanocomposite sensor films (Fig. 1)

$TiO_2$ nanocomposites with PANi were prepared by the addition of $TiO_2$ in different weight percentages (0–50%) in a smooth agate mortar and pestle. The nanocomposite powder was put in *m*-cresol and stirred for 11 h to get the casting solution. The thin films were prepared on glass substrates by the spin-coating method at 3000 rpm for 40 s and dried on a hot plate at 100°C for 10 min.[20] The silver paste strips 1 mm wide and 1 cm apart from each other were made on films for contacts. The thicknesses of the PANi emeraldine base (EB) film, $TiO_2$ film, and PANi–$TiO_2$ film were measured with a Dektak profilometer (Veeco, Santa Barbara, CA 93117) and were found to be 0.21, 0.29, and 0.32 μm, respectively.

## RESULTS AND DISCUSSION

### XRD analysis

Figure 2 shows the XRD patterns of the PANi, $TiO_2$, and PANi–$TiO_2$ nanocomposites (20–50 wt %) materials. The XRD pattern of PANi [Fig. 2(a)] showed a broad peak at 25.30°, which corresponded to the (110) plane of PANi.[18] The diffraction pattern of $TiO_2$ [Fig. 2(b)] showed sharp and well-defined peaks, which indicated the crystallinity of the synthesized material. The observed 2θ values were consistent with the standard joint commission powder diffraction standard (JCPDS) values (JCPDS No. 78-1285 and 86), which enumerated the mixed anatase (marked A in the figure) and rutile tetragonal (marked R in the figure) structures of $TiO_2$. No impurity phase was observed. The intensities of the diffraction peaks for the PANi–$TiO_2$ nanocomposites [Fig. 2(c)] were lower than that for $TiO_2$. The presence of amorphous PANi reduced the mass volume

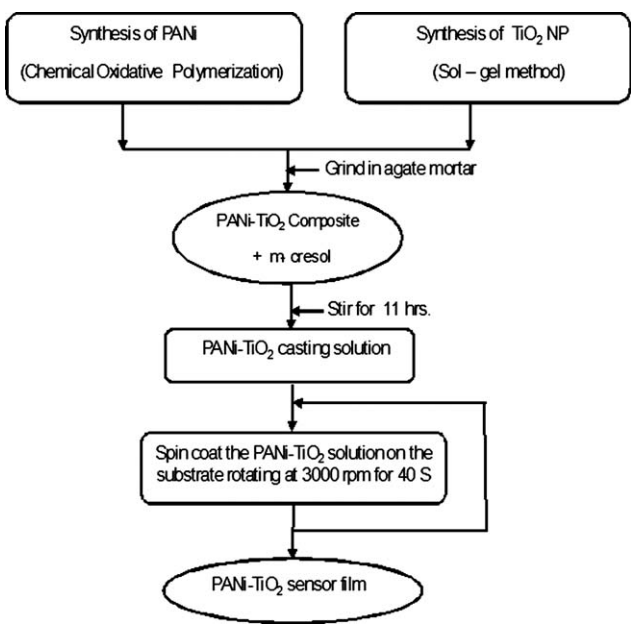


**Figure 1** Flow diagram of the synthesis of the PANi–$TiO_2$ thin-film sensor. (NP, Nanoparticles) (Veeco, Santa Barbara, CA 93117).

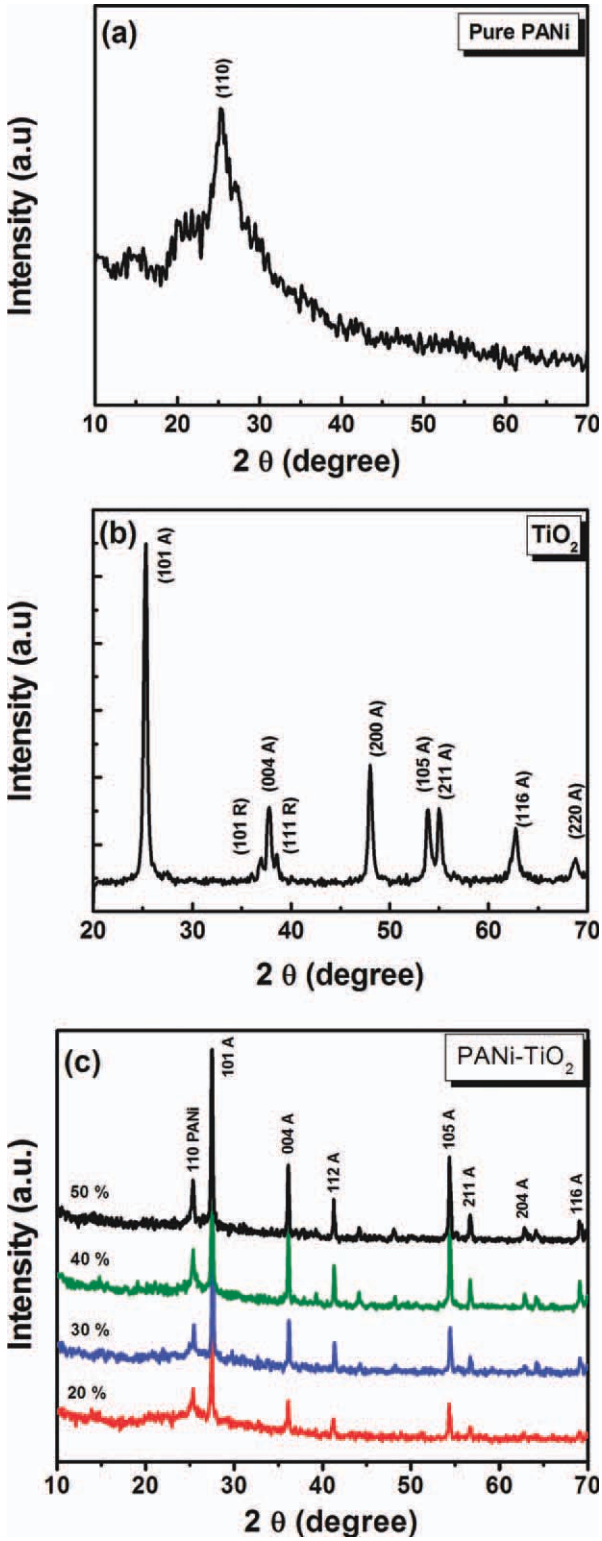


**Figure 2** XRD patterns of (a) pure PANi, (b) $TiO_2$, and (c) PANi–$TiO_2$ (20–50 wt %). [Color figure can be viewed in the online issue, which is available at wileyonlinelibrary.com.]

percentage of $TiO_2$ and sequentially weakened the diffraction peaks of $TiO_2$. It was also observed that the crystallinity of PANi was improved by the addition of $TiO_2$ nanoparticles. The XRD diffractograms of the PANi–$TiO_2$ nanocomposites showed that all of the major diffraction peaks of nanocrystalline $TiO_2$ were in the same peak angle positions. Because the nanocomposite films with 50% $TiO_2$ added showed maximum crystallinity, we carried out further studies on these films.

### Morphological analysis

Figure 3(a–f) shows the scanning electron micrographs of the PANi, PANi–$TiO_2$ (20–50 wt %), and $TiO_2$ films at x 20,000 magnification, respectively. The scanning electron microscopy image of the PANi film [Fig. 3(a)] exhibited a fibrous structure with many pores and gaps among the fibers. Figure 3(f) shows the surface morphology of the $TiO_2$ nanoparticle film annealed at 700°C for 1 h. The image shows that the nanoparticles were fine, with an average grain size of about 60 nm. The image of the nanocomposite [Fig. 3(b–e)] showed that there was no agglomeration or uniform distribution of the $TiO_2$ particles in the PANi matrix. We considered that the nanostructured $TiO_2$ particles embedded within the netlike structure were built by PANi chains.

Morphology plays an important role in the sensitivity of gas-sensing films. The grain sizes, structural formation, surface-to-volume ratio, and film thickness are important parameters for gas-sensing films. It could be seen that the PANi and PANi–$TiO_2$ (20–50%) films had a very porous structure, an interconnected network of fibers, and a high surface area. It has also been pointed out that such a structure contributes to a rapid diffusion of dopants into a film.

### FTIR spectroscopy analysis

The FTIR spectra of the PANi, PANi–$TiO_2$ (50 wt %) nanocomposite, and $TiO_2$ nanoparticles are shown in Figure 4. In the FTIR spectrum of the PANi–$TiO_2$ nanocomposite, we observed the presence of both Ti—O—Ti and PANi bands. The assignments of the various bands are given in Table I. A slight shift of the bands observed in the spectrum of PANi (e.g., at 1572 $cm^{-1}$ for the C=N stretching for the quinoid unit and at 1489 $cm^{-1}$ for the C=C stretching for benzenoid unit) indicated interaction between PANi and $TiO_2$.[16,20] However, the Ti—O—Ti band at 725 $cm^{-1}$ did not show much shifting. A small band at 1408 $cm^{-1}$ was also visible because of —OH, as reported.[16]

### UV–vis spectroscopy analysis

UV–vis spectra of the PANi, PANi–$TiO_2$ (50 wt %) nanocomposite, and $TiO_2$ nanoparticles are given in Figure 5. Three distinctive peaks of PANi appeared at about 336, 451, and 924 nm; these were attributed

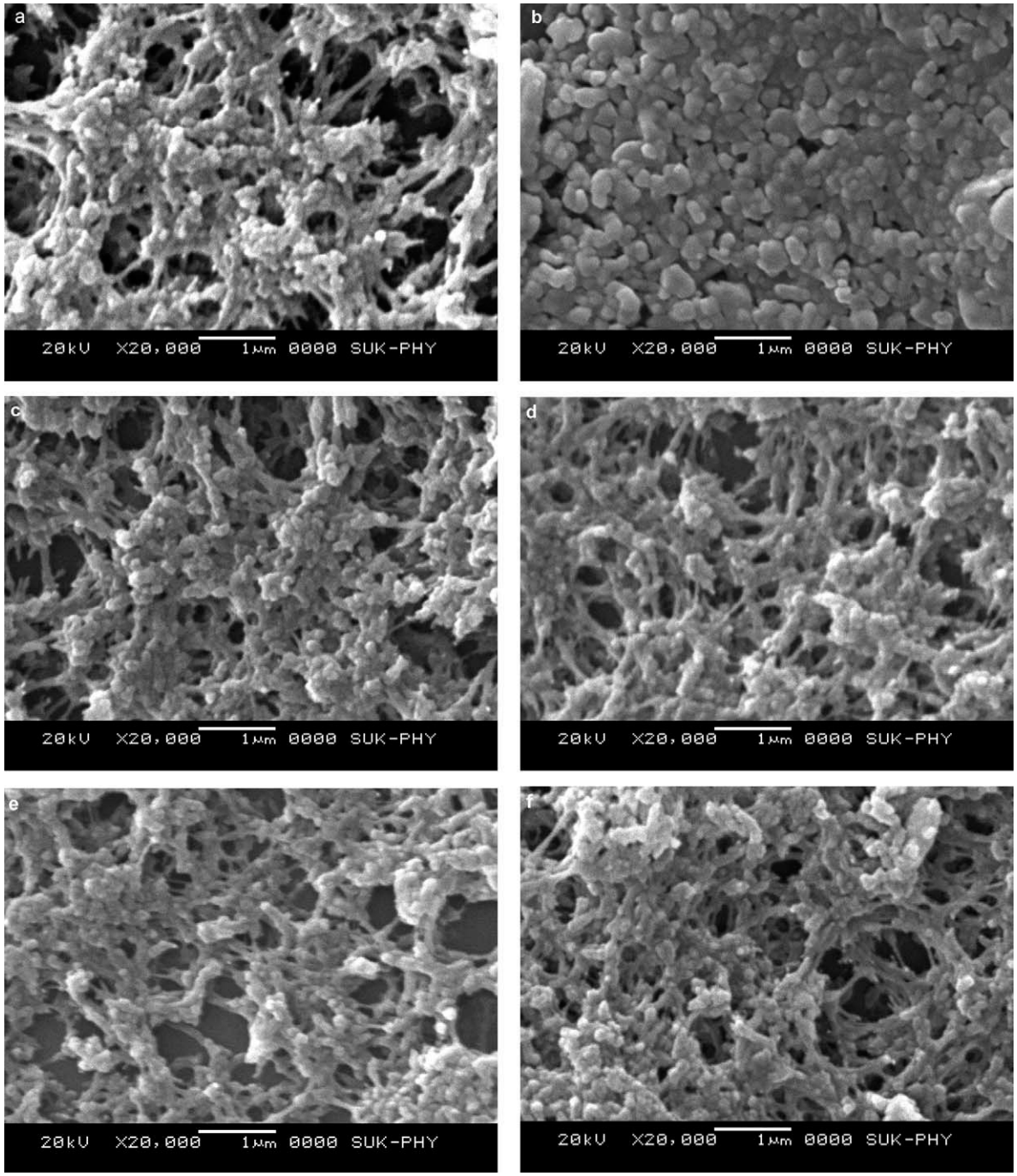


**Figure 3** Scanning electron micrographs of (a) PANi, (b) $TiO_2$, and (c) PANi–$TiO_2$ (50 wt %) films.

to the π–π*, polaron–π*, and π–polaron transitions, respectively. Also, two distinctive peaks of $TiO_2$ appeared at about 339 and 416 nm; these were attributed to the π–π* and polaron–π* transition, respectively.[20] From Figure 5, it can be noted that all of the characteristic peaks of the $TiO_2$ nanoparticles and PANi appeared in the PANi–$TiO_2$ nanocomposite. Moreover, the peak at 924 nm obviously shifted from 924 to 865 nm in the nanocomposite film. This indicated that the insertion of $TiO_2$ nanoparticles had an effect on the doping of conducting PANi, and this effect should have been due to an interaction at the interface of the PANi and $TiO_2$ nanoparticles.[20]

## Gas-sensing properties

To record responses to different gases, contacts were made on silver paste strips 1 mm wide and 1 cm apart from each other. The films deposited on the glass substrates were mounted in an airtight stainless steel (SS) housing of 250 cc, and a measured

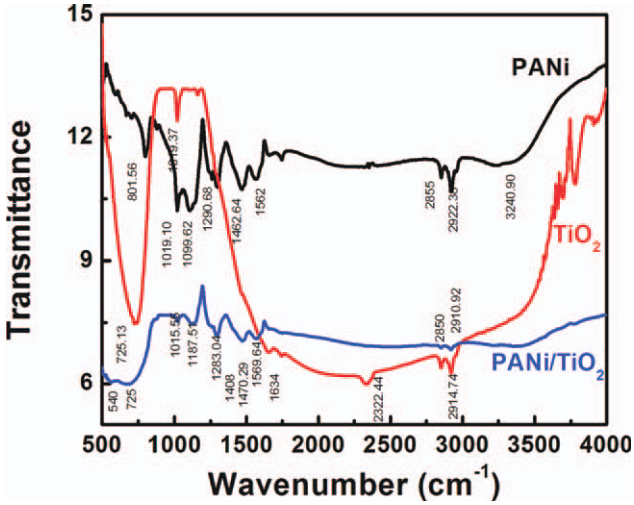


**Figure 4** FTIR spectra of (a) PANi, (b) nano-$TiO_2$, and (c) PANi/$TiO_2$ (50 wt %) films. [Color figure can be viewed in the online issue, which is available at wileyonlinelibrary.com.]

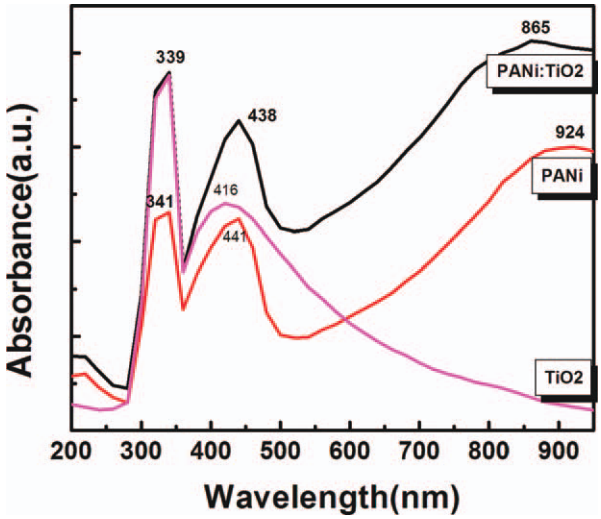


**Figure 5** UV–vis absorption spectra of the (a) PANi, (b) nano-$TiO_2$, and (c) PANi/$TiO_2$ (50 wt %) films. [Color figure can be viewed in the online issue, which is available at wileyonlinelibrary.com.]

quantity of desired gas (from a standard canister of 1000-ppm concentration) was injected through a syringe to yield the desired gas concentration in the housing. We measured the room-temperature gas response to various concentrations of different oxidizing and reducing (ammonia, ethanol, methanol, nitrogen dioxide, and hydrogen sulfide) gases by recording the resistances of the film in air and in the presence of any particular ambient. A Rigol 3062 ($6\frac{1}{2}$ digit) digital multimeter (DMM) (Beijing, China) was used to measure the resistance variations of the sensor films.

The sensor response ($S$; %) was defined as follows:

$$S = (Rg - Ra)/Ra \times 100\%$$

where $R_g$ and $R_a$ are the resistances of the sensor film in a measuring gas and in clean air, respectively.[15] The room-temperature gas-sensing measurement setup used is shown in Figure 6.

An attempt was made to study the selectivity of PANi–$TiO_2$ (50%) films for a lower concentration of $NH_3$ (20 ppm) compared to the sensitivities for higher concentrations of $CH_3$—OH, $C_2H_5$—OH, $NO_2$, and $H_2S$ (100 ppm). The bar chart for selectivity is as shown in Figure 7. It was observed that the PANi–$TiO_2$ thin films could sense a lower concentration of $NH_3$ with a higher sensitivity value compared to a large concentration of other gases. The plausible mechanism of selectivity for $NH_3$ could be traced to the characteristics of vapor adsorbed over the surface of the PANi–$TiO_2$ nanocomposite. In the case of gases used in this study, a comparison could be made from the electron affinity values ($NH_3$: 211.3 kcal/mol, NO: 1.25 kcal/mol, and $H_2S$: 50.4

**TABLE I**
**Characteristic Frequencies of the PANi/$TiO_2$ Nanocomposites**

| Wave number ($cm^{-1}$) | Assignment |
|---|---|
| 3225–3451 | N—H stretching of aromatic amines |
| 2845–2914 | C—H stretching of aromatic amines |
| 504 | C—H out-of-plane bending vibration |
| 1572 | C=N stretching mode vibration for the quinoid unit |
| 1489 | C=C stretching mode vibration for the benzenoid unit |
| 1296 and 1239 | C—N stretching mode of the benzenoid ring |
| 1000–1115 | C—H in-plane bending vibration |
| 797 | C—H out-of-plane bending vibration |
| 725 | Ti—O—Ti antisymmetric vibration |

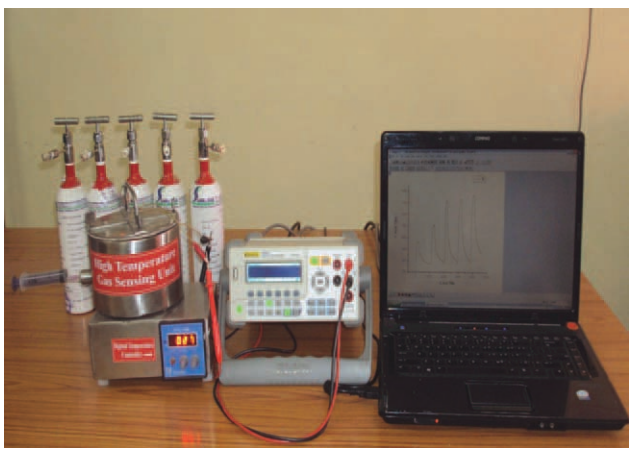

**Figure 6** Gas-sensing measurement setup. [Color figure can be viewed in the online issue, which is available at wileyonlinelibrary.com.]

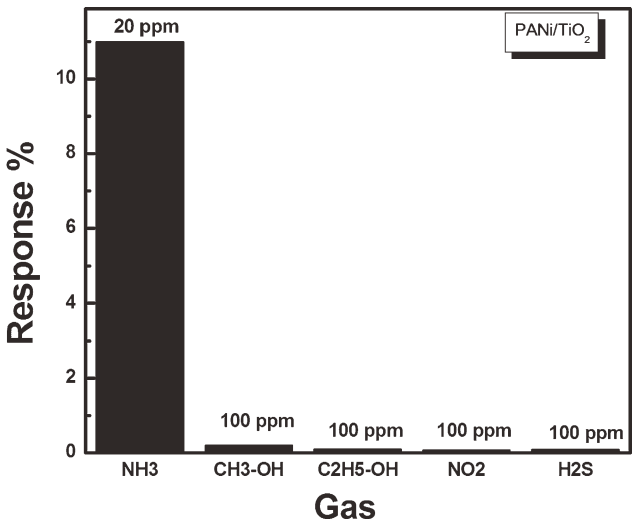


**Figure 7** Gas responses of the PANi–$TiO_2$ sensor film to 20 ppm of $NH_3$ and 100 ppm of $CH_3$—OH, $C_2H_5$—OH, $NO_2$, and $H_2S$.

kcal/mol) of individual gases.[21] The difference in sensitivities to different gases might have been due to this phenomenon.

We compared the sensitivity of the PANi–$TiO_2$ (50%) nanocomposite toward 100-ppm $NH_3$ with that of the pure PANi and pure $TiO_2$ films, as shown in Figure 8.

It was observed that $TiO_2$ showed an *n*-type response with a decrease in its resistance on exposure to $NH_3$ gas. However, it did not show any response at room temperature and had to be operated at 200°C. In the case of the pure PANi film, the resistance increased on exposure to $NH_3$, but the response was quite smaller compared to that in the PANi–$TiO_2$ composite. This showed that the nanocomposite film was best suitable for the detection of $NH_3$ gas at room temperature. To explain the higher response and gas-sensing mechanism of the PANi–$TiO_2$ nanocomposite, Tai et al.[15] postulated that PANi and $TiO_2$ may form a *p*–*n* junction, and the observed increased response of the nanocomposite material may have been due to the creation of a positively charged depletion layer on the surface of $TiO_2$, which could be formed because of interparticle electron migration from $TiO_2$ to PANi at the heterojunction. This would cause the reduction of the activation energy and enthalpy of physisorption for $NH_3$ gas.

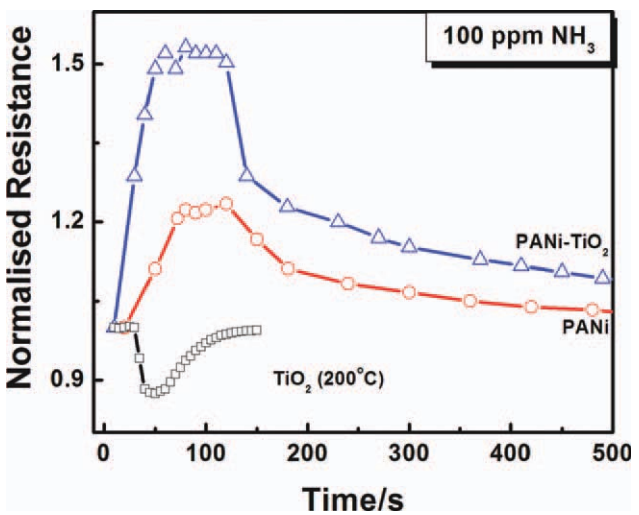


**Figure 8** Response of the (a) pure $TiO_2$, (b) pure PANi, and (c) nanocomposite of the PANi–$TiO_2$ film toward 100-ppm $NH_3$ gas at room temperature. [Color figure can be viewed in the online issue, which is available at wileyonlinelibrary.com.]

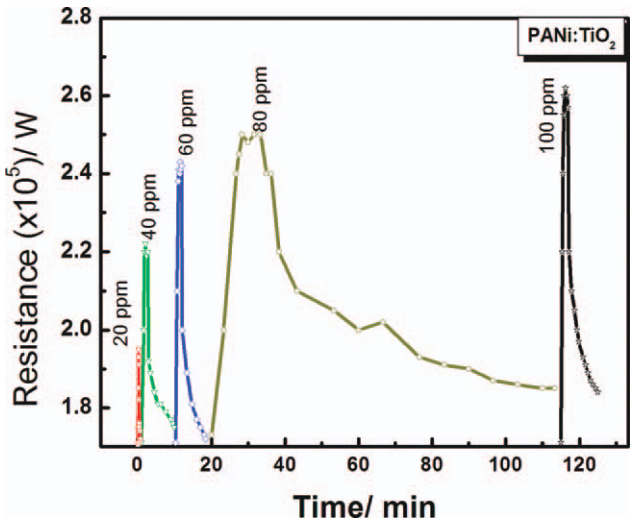


**Figure 9** Gas responses–recovery curve of the PANi–$TiO_2$ sensor films to different concentrations of $NH_3$. [Color figure can be viewed in the online issue, which is available at wileyonlinelibrary.com.]

The sensing capability of the PANi–$TiO_2$ nanocomposite sensors toward different concentrations (20–100 ppm) of ammonia vapor were explored. Figure 9

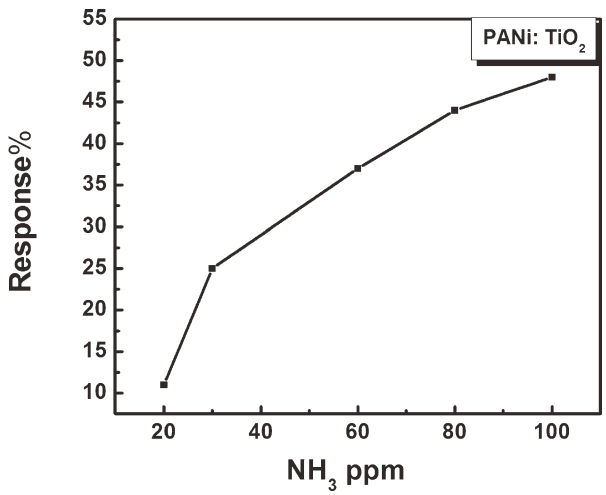


**Figure 10** Response of the PANi–$TiO_2$ thin-film sensor to $NH_3$ (20–100 ppm).

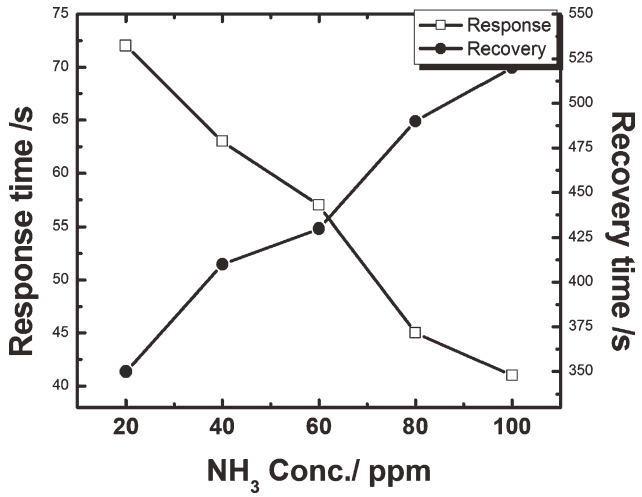


**Figure 11** Variation of the response and recovery times of the PANi–$TiO_2$ thin-film sensor with $NH_3$ concentration.

shows the electrical response of the PANi–$TiO_2$ films to 20, 40, 60, 80, and 100 ppm $NH_3$. The resistance increased dramatically upon exposure to ammonia vapor, attained a stable value, and decreased gradually after the film was transferred to clean air. The increase in resistance after exposure to $NH_3$ may have been due to the porous structure of the PANi–$TiO_2$ films; this led to the predominance of surface phenomena over bulk material phenomena. The surface adsorption (chemisorptions) of $NH_3$ may have led to the formation of ammonium. The resistance attained a stable value when dynamic equilibrium was attained.[16] The response values of the PANi–$TiO_2$ sensor films are plotted as a function of the $NH_3$ concentration in Figure 10. It was observed that the response was saturated at higher concentration; this may have been due to a lower availability of surface area with possible reaction sites on the surface of the film.

The response/recovery time is an important parameter for characterizing a sensor. The response time and recovery time are defined as the times of 90% total resistance change.[12] Figure 11 shows the response and recovery times of PANi–$TiO_2$ for different concentrations of $NH_3$. It was revealed that the response time decreased from 72 to 41 s when the $NH_3$ concentration increased from 20 to 100 ppm. This may have been because of the higher diffusion rate of a higher concentration into the film surface. The porous structure of the exposed film facilitated the rapid diffusion of gas molecules into the bulk. From the same graph, it was found that for a higher concentration of $NH_3$, the recovery time was longer. This may have been due to lower desorption rate of the reaction products from the surface.

## CONCLUSIONS

Nanostructured PANi–$TiO_2$ (0–50%) thin-film sensors were fabricated by a spin-coating technique onto a glass substrate operating at room temperature. It was observed that the PANi–$TiO_2$ film had a very porous structure, an interconnected network of fibers, and a high surface area; these contributed to the rapid diffusion of dopants into the film. FTIR and UV analysis revealed the insertion of $TiO_2$ nanoparticles into the PANi matrix. The response behavior observed for the PANi–$TiO_2$ nanocomposite thin films revealed higher sensitivity values and faster response and recovery rates to ammonia compared to those of pure PANi and $TiO_2$.

The gas-sensing properties of the PANi–$TiO_2$ thin films to ammonia and other gases, such as $NO_2$, $H_2S$, and so on, indicated that the PANi–$TiO_2$ thin films are an excellent candidate for ammonia recognition at room temperature.

## References

1. Prasad, G. K.; Radhakrishnan, T. P.; Sravan Kumar, D.; Ghanshyam Krishna, M. Sens Actuators B 2005, 106, 626.
2. Wrenn, C. Occup Health Saf 2000, 69, 64.
3. Chandrakanthi, R. L. N.; Careem, M. A. Thin Solid Films 2002, 417, 51.
4. Somani, P. R.; Marimuthu, R.; Mulik, U. P.; Mulik, S. R.; Sanikar, S. R.; Amalnerkar, D. P. Synth Met 1999, 106, 45.
5. He, Y. Mater Chem Phys 2005, 92, 134.
6. Chen, S. A.; Chuang, K. R.; Chao, C. I.; Lee, H. T. Synth Met 1996, 82, 207.
7. MacDiarmid, A. G.; Yang, L. S.; Huang, W. S.; Humphrey, B. D. Synth Met 1987, 18, 393.
8. Verma, D.; Datta, V. Sens Actuators B 2008, 134, 373.
9. Mastuguchi, M.; Okamoto, A.; Sakai, Y. Sens Actuators B 2003, 94, 46.
10. Chaung, F. Y.; Yang, S. M. Synth Met 2005, 152, 361.
11. Sadek, A. Z.; Wlodarski, W.; Shin, K.; Bkaner, R.; Kalantar-Zadeh, K. Nanotechnology 2006, 17, 4488.
12. Dhawale, D. S.; Salunkhe, R. R.; Patil, U. M.; Gurav, K. V.; More, A. M.; Lokhande, C. D. Sens Actuators B 2008, 134, 988.
13. Geng, L.; Zhao, Y.; Huang, X.; Wang, S.; Zhang, S.; Wu, S. Sens Actuators B 2007, 120, 568.
14. Parvatikar, N.; Jain, S.; Khasim, S.; Ravansiddappa, M.; Bhoraskar, S. V.; Ambikaprasad, M. V. N. Thin Solid Films 2006, 514, 329.
15. Tai, H.; Juang, Y.; Xie, G.; Yu, J.; Chen, X. Sens Actuators B 2007, 125, 664.
16. Tai, H.; Juang, Y.; Xie, G.; Yu, J.; Chen, X.; Ying, Z. Sens Actuators B 2008, 129, 319.
17. Gong, J.; Li, Y.; Hu, Z.; Zhou, Z.; Deng, Y. J Phys Chem C 2010, 114, 9970.
18. Pawar, S. G.; Patil, S. L.; Mane, A. T.; Raut, B. T.; Patil, V. B. Arch Appl Sci Res 2009, 1, 109.
19. Pawar, S. G.; Patil, S. L.; Chougule, M. A.; Jundale, D. M.; Patil, V. B. J Mater Sci Mater Electron 2011, 22, 260.
20. Pawar, S. G.; Patil, S. L.; Chougule, M. A.; Mane, A. T.; Jundale, D. M.; Patil, V. B. Int J Polym Mater 2010, 59, 777.
21. Joshi, A. Ph.D. Thesis, University of Pune, 2010.